Physicochemical Properties of Fluorinated Diamond Electrodes

Sergio Ferro and Achille De Battisti*

Department of Chemistry, University of Ferrara, via L. Borsari 46, I-44100 Ferrara, Italy

Received: November 11, 2002; In Final Form: March 4, 2003

Although boron-doped diamond (BDD) is itself quite stable and chemically inert, some electrochemical applications could require further improvement, and fluorination could be one of the most promising methods. In the present paper, a characterization of diamond film electrodes surface-modified by fluorine insertion, through CF_4 plasma treatment, has been carried out. X-ray photoelectron spectroscopy (XPS) analysis showed that the above preparation method most probably leads to the fluorination of the near-surface region of the diamond film. The electrochemical characterization showed that the fluorination of BDD shifts the cathodic water decomposition by about 2 V in the negative direction; this behavior could not be ascribed to problems of film conductivity and/or to a decrease in electronic density of states. The electron-transfer kinetics for model redox couples such as the Eu^{3+}/ Eu^{2+}, Fe^{3+}/Fe^{2+}, and ferri/ferro cyanide redox systems has been found to be quite significantly affected by the surface modification, while the electrochemical behavior of methyl viologen remains practically unchanged. The exchange current densities for the aquo complexes are decreased about five times, while for the cyano complex of more than 3 orders of magnitude.

Introduction

The rapid development of different techniques for the synthesis of diamond[1] has attracted the interest of many researchers, more and more applications being suggested for this outstanding material. In most cases, the synthesis is focused on the formation of a thin film, to supply the supporting material with otherwise unattainable physical properties. It is well-known that diamond is the hardest material and has a great chemical inertness; nevertheless, the modification of the outer surface of the diamond film may open new possibilities, also in terms of an increased stability. In this context, fluorine appears to be a promising modifier,[2] the stability and the inertness of some perfluorinated compounds (Teflon, Kalrez) having already found industrial applications. To form such a monolayer, different approaches can be followed, as summarized in the Smentkowski and Yates' patent,[2] although with different results (in terms of fluorine coverage).

Dealing with a conducting diamond film, modifications of the outer surface are expected to change also the electrochemical properties of the device under investigation. Angus and co-workers[3] carried out voltammetry and X-ray photoelectron spectroscopy (XPS) analysis to show that the fluorination of the diamond surface is able to "passivate" the graphitic impurities that are present at the grain borders of polycrystalline diamond films. The investigation was carried out in 0.5 M sulfuric acid and only a few cyclic voltametry (CV) curves were recorded.

The present work is thus devoted to a deeper investigation of the electrochemical properties of fluorinated diamond thin films. The use of different redox couples is common practice for the characterization of an electrode material: in a previous work, we used both the iron(III)/iron(II) and the ferri/ferro cyanide redox equilibria to describe the electrochemical properties of highly boron-doped (BDD) electrodes (see ref 4 and references therein). The obtained results showed that high-quality BDD specimens behave like the usual (oxide-free) noble-metal electrodes, if care is devoted to the preparation of solutions, to avoid the presence of species which adsorb onto the electrode surface or are able to catalyze the electron-transfer reaction.

Experiments have been carried out making use of fluorinated BDD electrodes, synthesized at CSEM (Neuchâtel, Switzerland) by plasma-treating the pristine BDD samples in a CF_4 atmosphere.

Experimental Section

Commercially available BDD electrodes, synthesized at CSEM by the hot filament chemical vapor deposition technique (HFCVD) on *p*-type, low-resistivity (1/3 mΩ·cm), {100} silicon wafers (Siltronix; diameter, 10 cm; thickness, 1.0 mm), have been used. The plasma−fluorination reaction was performed at CSEM using CF_4 as the reactive gas, in a microwave plasma reactor at 13.56 MHz. The pristine BDD film had a thickness of 1 μm ($\pm$10%) and a resistivity of 15 mΩ·cm ($\pm$30%), consistent with a boron concentration between 3500 and 5000 ppm.

Different morphological characterizations of the fluorinated BDD films have been carried out; scanning electron microscopy (SEM) investigations were performed using a Stereoscan S360 from Cambridge Instruments; a Nanoscope IIIa scanning probe microscope controller, connected with a Nanoscope Multimode SPM, both from Digital Instruments, were adopted for atomic force microscopy (AFM) analysis. C1s, O1s, F1s, and Si2p X-ray photoelectron spectra were recorded using a VG Scientific ESCALAB MkII, which operated in constant analyzer energy mode, at a pass energy of 50 eV for wide-scan survey spectra and 20 eV for higher energy resolution region scans. A nonmonochromatized Mg Kα source operating at 300 W (20 mA, 15 kV) was used, and the takeoff angle, selected to 0° (normal angle, $\perp$) or 70° (grazing angle, $\angle$); measurements were performed at a pressure of 1×10^{-9} mbar. The obtained

* To whom correspondence should be addressed. FAX: +39 0532 240709. E-mail address: dba@dns.unife.it.

10.1021/jp0274280 CCC: $25.00
Published on Web 07/03/2003

information is limited by the maximum analyzing depth, which is strictly dependent on the anelastic mean free path of photoelectrons: in our case, the analyzed sample thickness is between 10 and 100 Å.

Electrochemical measurements were performed with an Autolab PGSTAT20 (EcoChemie), housing the BDD electrode at the bottom of the electrolysis cell (which was made of Teflon and glass), with only the diamond thin film surface (0.785 cm^2, i.e., a disk with a diameter of 1 cm) in contact with the electrolyte solution. A cylindrical platinum grid or a piece of carbon felt were used as the counter electrode, and potentials were recorded against a double-walled saturated calomel electrode (SCE), with an intermediate saturated $NaNO_3$ solution. For the measurements carried out at different temperatures, a non-isothermal reference electrode cell (liquid junction connection, equipped with a three-way stopcock) was adopted, which allowed minimization of the thermal liquid-junction potential (<ca. 1 mV).[5]

Solutions of 5 mM, containing both the reduced and the oxidized form of the ions under investigation, were prepared with MilliQ water (ρ >18 MΩ·cm), using analytical grade, hydrate reagents. $Fe(ClO_4)_2$, $Fe(ClO_4)_3$ (chloride < 0.005%), $K_4Fe(CN)_6$, and $K_3Fe(CN)_6$ were supplied by Aldrich and used without further purification. 1 M $HClO_4$ (Fluka) was adopted as background electrolyte for the iron(III)/iron(II) redox system, while both 0.5 M H_2SO_4 (Riedel-de Haën) and 1 M HCl (Riedel-de Haën) were adopted for the ferri/ferro cyanide redox couple. Eu_2O_3 (99.9%, Alfa Aesar) and methyl viologen dichloride hydrate (Aldrich) were used as received, while $EuCO_3$ has been synthesized on purpose. A 10 mM solution of both Eu(III) and Eu(II) was prepared as described in ref. 6; while not strictly important in the case of the present study, the pH was maintained at a value of 3, to allow a comparison with our previous results.[6] Similarly, a 0.5 mM solution of MV^{2+} in 1 M NaCl (Fluka) was prepared, to compare the results with those of the literature.[7,8]

Initial cyclic voltammetric curves were performed at room temperature and at different scan rates, between 0.01 and 1 V s^{-1}; the chosen potential range was cycled using a step potential of 2 mV and repeating the measure at least 3 times. In every case, the last cycle was recorded, although reproducible signals were obtained just after the first measure.

Quasi-steady polarization curves were carried out at a scan rate of 0.1 mV s^{-1} and with a step potential of 0.15 mV; curves were recorded in a range of ±30 mV with respect to the open circuit potential (OCP), starting from the higher value and conditioning the electrode at the initial potential for 30 s.

Electrochemical impedance spectroscopy was carried out by an Autolab frequency response analyzer (FRA), performing measurements at the OCP, in the 10^{-1}−10^4 Hz frequency range and with a measuring signal amplitude of 5 mV.

Some of the measurements carried out at room temperature. have been afterward performed at different temperatures, from ~5 to 60/70 °C, changing the temperature of the measuring solution by means of a thin-walled glass spiral tube in which cold or warm water was circulated; the temperature inside the cell was thus controlled within ±0.2 °C. The temperature variation involved only the working and the counter electrodes, as discussed above.

All DC data have been corrected for the ohmic drop on the basis of the uncompensated resistance determined by the impedance analysis.

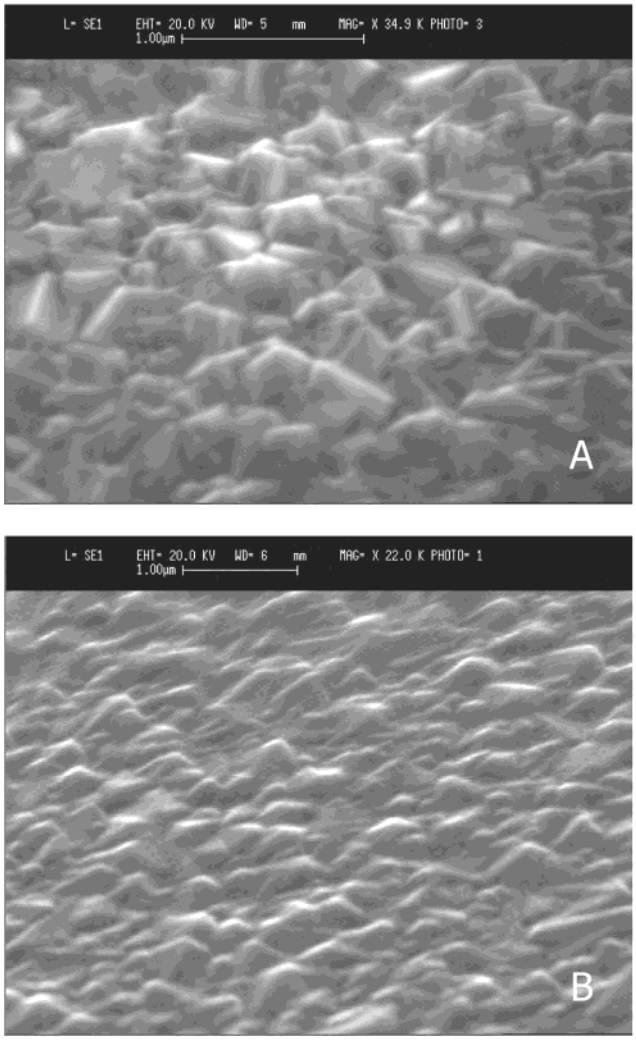

Figure 1. Scanning electron microscopy images of a pristine BDD sample (A) and a fluorinated one (B).

Results and Discussion

SEM images of both a hydrogen-terminated and a fluorinated diamond (F−BDD) surface are reported in Figure 1. Figure 1A shows that the boron-doped diamond layer is continuous and consists of randomly arranged microcrystals; their size varies approximately from 0.1 to 0.5 μm, and the facets are mainly ⟨111⟩ oriented, with some ⟨100⟩ orientation; twinning can be also observed on some crystals. On the other hand, the morphology of the fluorinated BDD specimen can be observed in picture 1B: crystals seem to be eroded by the plasma treatment, both the roughness and the real surface being therefore reduced.

Since the fluorination probably affects the conductivity at the surface, the investigation has been repeated by using AFM, a technique that does not need the sample to be electrically conductive. As shown in Figure 2, greater magnifications could be obtained; the shape of the fluorinated BDD crystals (Figure 2B) is still more rounded, evidence that some sort of erosion has taken place during the plasma treatment or that some material has been added.

X-ray photoelectron spectra confirm the presence of a fluorinated diamond layer at the surface of the investigated specimens. As shown in Figure 3A, the C1s peak of the unmodified BDD sample (dotted line) is observed at about 284 eV (the $Au4f_{7/2}$ signal at 83.7 eV of a thin gold layer, deposited

TABLE 1: Relative Abundances (%) Calculated from Peak Areas

	sample as received		sample after ultrahigh-vacuum treatment	
	normal angle, ⊥	grazing angle, ∠	normal angle, ⊥	grazing angle, ∠
C (%)	72.98	73.18	78.95	76.94
O (%)	8.40	8.72	8.51	8.97
F (%)	17.84	17.35	11.70	13.37
Si (%)	0.78	0.76	0.84	0.72
F/C	0.24	0.24	0.15	0.17

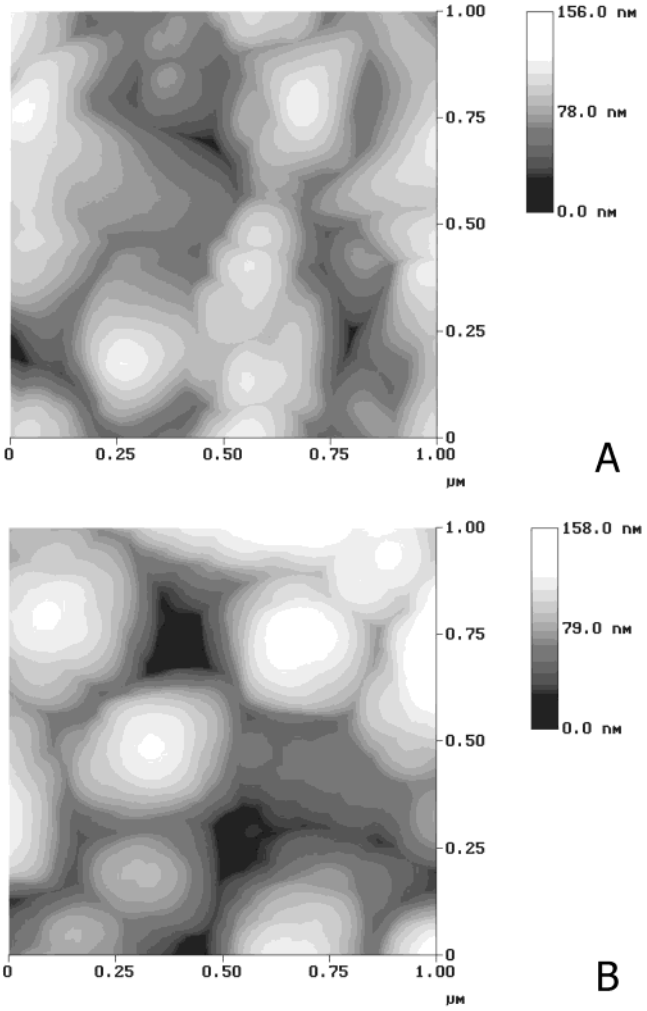

Figure 2. Atomic force microscopy images of the pristine and fluorinated BDD specimens of Figure 1.

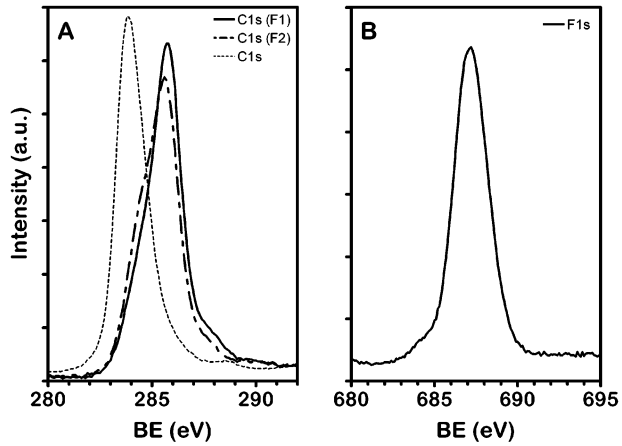

Figure 3. (A) C1s X-ray photoelectron spectra of a pristine BDD surface (dotted line) and a fluorinated BDD specimen, before (solid line) and after (broken line) a prolonged ultrahigh-vacuum treatment (see text for details).

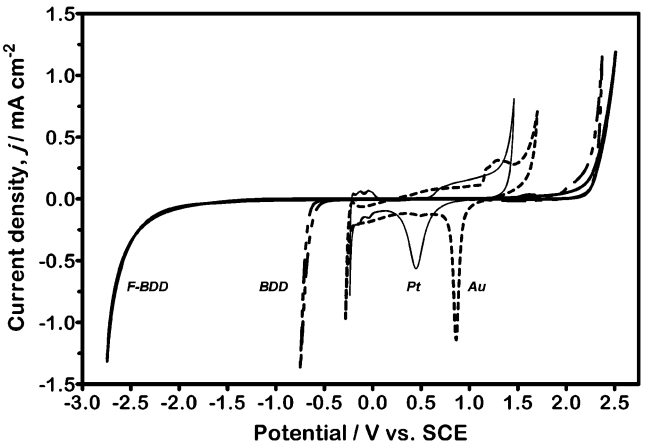

Figure 4. Comparison of CV curves for BDD, fluorinated BDD, platinum, and gold electrodes, in 1 M $HClO_4$. Scan rate: 0.2 V s^{-1}.

on the sample surface, has been used for calibration), while it shifts to higher bond energy (BE; +1.5 eV) at the fluorinated specimen (solid line). Referring again to Figure 3A, the broken line was also obtained at the fluorinated BDD sample, but after a 3 week period under ultrahigh vacuum ($\sim 10^{-9}$ mbar): both the decrease in intensity of the peak maximum and the broadening at low BE values suggest that at least part of the fluorination is not indefinitely stable and a very slow defluorination takes place. In addition, on the basis of a preliminary quantitative analysis (see Table 1), it seems that the fluorinated compounds are homogeneously distributed along the analyzed volume, instead of being localized only at the surface. Considering the experimental conditions for the modification, the possibility of a fluorination concomitant with film growth cannot be ruled out.

To complete the XPS characterization, Figure 3B shows the region relative to the F1s signal; while a precise resolution of overlapping peaks has not been carried out yet, the dominant component can be localized at about 687.2 eV. A second chemical species is possibly present at lower BE, but its intensity has been estimated to be less than 5%, with respect to the first one. Taking into consideration the paper by Foord and coworkers,[9] who studied the interaction of XeF_2 at chemical vapor deposited, polycrystalline diamond surfaces, the higher BE component could be attributed to a semiionic fluorine, the other species being related to covalently bonded carbon monofluoride functionalities.

To see how the fluorination modifies the electrochemical properties of the diamond surface, a series of blank cyclic voltammograms were recorded in 1 M $HClO_4$ prior to redox couples investigation. As is known, high-quality BDD films have a wide potential window of about 3 V without significant water decomposition.[6,10,11] As shown in Figure 4, the F−BDD electrode allows exploration of potential values about 2 V more negative, thus enlarging the window of polarizability to about 5 V (curves have been corrected for the ohmic drop).

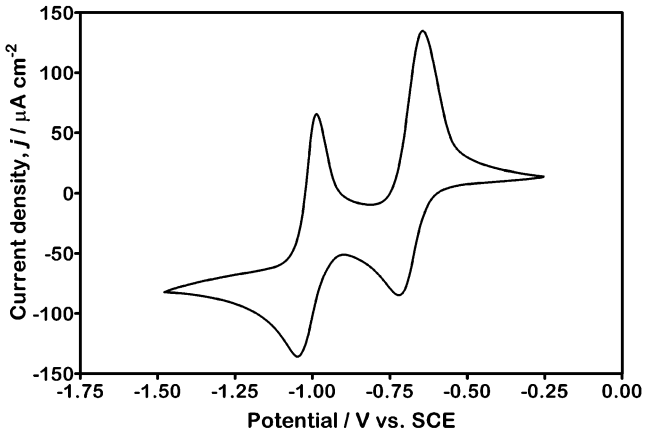

Figure 5. CV curve for 0.5 mM methyl viologen (MV^{2+}) in 1 M NaCl, recorded at the fluorinated BDD electrode (room temperature). Scan rate: 0.1 V s^{-1}.

Such behavior cannot be univocally rationalized, on the basis of the very few data so far available on the hydrogen evolution reaction (HER) at conductive diamond electrodes.[12] A possible mechanism for the HER at hydrogen-terminated diamond electrodes hypothesizes a strong interaction between the proton and the hydrogen-terminated surface, which should result in the abstraction of surface hydrogen atoms:

$$C{-}H + H^+ + e \rightarrow C\bullet + H_2$$

Notwithstanding the validity of this mechanism, it is clearly not applicable to the present case, where the surface is fluorine-terminated. According to Martin and collaborators,[12] an alternative could be the direct liberation of atomic hydrogen ($H^+ + e \rightarrow H$), whose standard reduction potential is $E^\circ = -2.11$ V, quite in accordance with the onset of the HER as reported in Figure 4 (with reference to the SCE).

Another possibility could be related to changes in electronic density of states coming from particular interactions between the fluorine and the carbon and/or boron atoms in the near-surface region of the diamond film. The investigation has been thus carried out by analyzing the electrochemical behavior of the methyl viologen (MV^{2+}) and Eu^{3+}/Eu^{2+} redox systems. The former, in particular, is known as an analyte whose electrochemical kinetics is relatively insensitive to the nature of the electrode surface and depends only on the local density of electronic states at the formal potentials of the redox reaction.[8]

A typical CV curve for a 0.5 mM MV^{2+} solution in 1 M NaCl, obtained at room temperature and at a 0.1 V s^{-1} scan rate, is reported in Figure 5. Formal reduction potentials of -0.684 and -1.018 V have been obtained, related to the $MV^{2+}/MV\bullet^+$ and $MV\bullet^+/MV^0$ redox equilibria, respectively, while the ΔE_p values are 77 and 62 mV, in that order. These near-Nernstian values indicate a sufficient density of states, i.e., the fluorinated diamond electrode behaves as a semimetal, at these potentials, not as a semiconductor (also the possibility of a current rectification has to be excluded).

Further information has been attained from the investigation of the Eu^{3+}/Eu^{2+} redox system; the CV signal of a 10 mM solution of this redox couple, recorded at the F−BDD electrode, is reported in Figure 6, together with analogous signals, previously obtained at "as grown" and "oxidized" BDD electrodes.[6] The possibility to explore more cathodic potential values, without a significant contribution from the HER, is beneficial for the investigation: the reduction process can be properly recorded, while in ref 6 the cathodic limit was not a completely free choice. As far as the electrochemical kinetics is concerned, the Eu^{3+}/Eu^{2+} redox couple behaves even more irreversibly than previously observed;[6] in more details, a kinetic constant value of $(5.1 \pm 0.9) \times 10^{-7}$ cm s^{-1} was obtained, from the slope of $j-E$ profiles (low-overpotential approximation) and polarization resistances, R_p, obtained by impedance measurements. These data have to be compared with those obtained under similar conditions but at as grown and oxidized BDD electrodes: apparent kinetic constant values were respectively equal to $(2.7 \pm 0.5) \times 10^{-6}$ and $(4.3 \pm 0.6) \times 10^{-6}$ cm s^{-1}, suggesting slightly faster kinetics at more hydrophilic electrode surfaces.

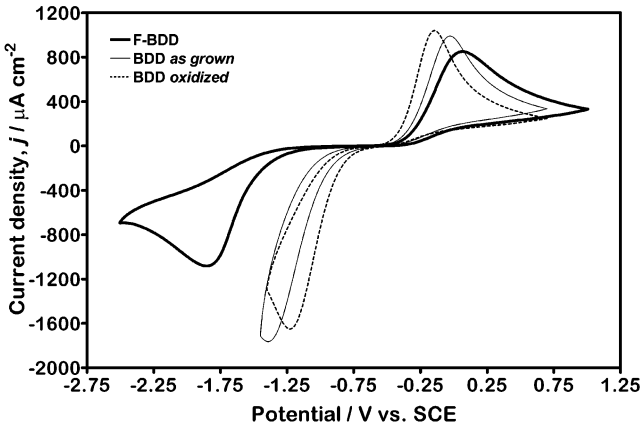

Figure 6. CV curves for 10 mM $Eu^{3+/2+}$ in 0.001 M $HClO_4$/0.999 M $NaClO_4$ at the fluorinated BDD electrode (comparison with data obtained at *as grown* and *oxidized* BDD[6]). Room temperature; scan rate, 0.1 V s^{-1}.

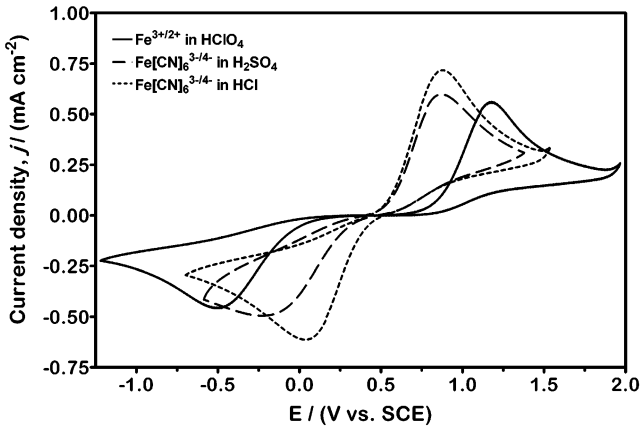

Figure 7. CV curves for the $Fe^{3+/2+}$ (5 mM, in 1 M $HClO_4$) and $Fe[CN]_6^{3-/4-}$ (5 mM, in 0.5 M H_2SO_4 and 1 M HCl) redox couples, recorded at the fluorinated BDD electrode (room temperature). Scan rate: 0.1 V s^{-1}. Apparent kinetic constant values are $(5.4 \pm 0.4) \times 10^{-7}$, $(1.2 \pm 0.1) \times 10^{-5}$, and $(2.6 \pm 0.5) \times 10^{-5}$ cm s^{-1}, respectively.

Moving away from the negative potential values, most of the electrochemical characterization has been carried out considering the two redox couples of iron; Figure 7 shows CV curves for Fe^{3+}/Fe^{2+} in $HClO_4$ and $Fe[CN]_6^{3-}/Fe[CN]_6^{4-}$ in the two different media (H_2SO_4 and HCl), obtained at room temperature and at a 0.1 V s^{-1} scan rate. All three systems behave quite irreversibly; in addition, the supporting electrolyte anion clearly plays a significant role in determining the reversibility of the ferri/ferro cyanide redox couple (the rate constant increases in the series $F^- < CNS^- < SO_4^{2-} < CH_3COO^- < ClO_4^- < PO_4^{3-} < NO_3^- < Cl^- < Br^-$, as reported by Galus et al. at Pt electrodes[13]). Such an effect was not previously observed at BDD:[4] in that case, in fact, the ferri/ferro cyanide system was

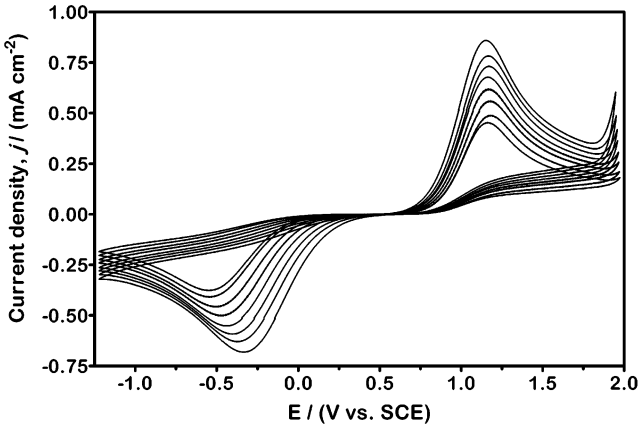

Figure 8. CV curves for 5 mM $Fe^{3+/2+}$ in 1 M $HClO_4$ at different temperatures (from 5 to 70 °C), at the fluorinated BDD electrode. Scan rate: 0.1 V s^{-1}.

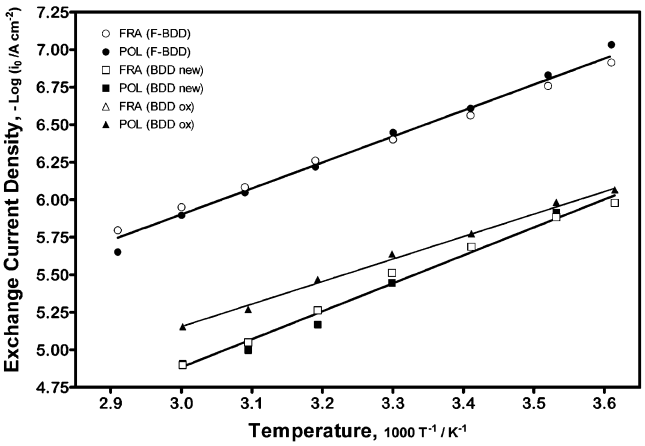

Figure 9. "Arrhenius plot" for the $Fe^{3+/2+}$ redox couple (comparison with data obtained at *as grown* and *oxidized* BDD[4]).

found to have a perfectly reversible behavior, despite the fact that measurements were carried out in sulfuric media (which stays at an initial position in the above series).

To better elucidate the processes, the role of temperature has been considered, changing its value in the range from about 5 to 60 °C (70 °C in the case of Fe^{3+}/Fe^{2+}). Results for the iron(III)/iron(II) redox couple are given in Figure 8 in terms of cyclic voltammetries, while the kinetic data (obtained by the low-overpotential approximation and the impedance analysis) are elaborated in terms of the "Arrhenius plot" in Figure 9, where they are compared with those obtained at as grown (new, hydrophobic) and oxidized (ox., hydrophilic) BDD electrodes.[4] At the fluorinated BDD, the activation enthalpy result is 7.92 ± 0.22 kcal mol^{-1}, while it was 8.53 ± 0.27 and 6.86 ± 0.16 kcal mol^{-1} in the other two cases, respectively. Clearly, the redox couple behaves similarly at the two hydrophobic surfaces, at least as far as the activation enthalpy is concerned. Referring to the intercept of the plot of ln i_0 vs $1/T$ (at $1/T \rightarrow 0$), we stressed in ref 4 that it is not directly a measure of the entropy of activation ($\Delta S^{\circ\ddagger}$), a contribution arising from the preexponential factor of the Arrhenius law being present. More in detail, expressing the preexponential factor in terms of the rotational, vibrational, and electronic properties of species (reagents and activated complex), a significant difference in electronic contributions should be present for the two electrode materials (F−BDD and BDD), as a consequence of the present surface modification (fluorination). Accordingly, it is difficult to assign the difference between the two intercepts (+0.710 ± 0.160 vs −0.705 ± 0.196) to a difference in $\Delta S^{\circ\ddagger}$: however, if this would be the case, a more negative variation of the activation entropy would accompany the electrochemical reaction (which is tacitly assumed to be the oxidation of Fe^{2+}) taking place at the fluorinated BDD electrode.

Analogous investigations have been carried out for the ferri/ferro cyanide redox couple, in the two acidic media. The role of the anion of the supporting electrolyte can be appreciated again, comparing the impedance data (recorded at different temperatures) shown in Figure 10 (lower polarization resistance values were measured in the HCl media, Figure 10B, compared to the sulfuric one, Figure 10A). Again, the data previously obtained at BDD (as grown and oxidized, ref 4) have been taken into consideration against those presently obtained at the fluorinated BDD electrode, reporting the comparison in terms of an Arrhenius plot, as shown in Figure 11. Activation enthalpies ($\Delta H^{\circ\ddagger}$) of 1.78 ± 0.09, 1.28 ± 0.14, and 3.99 ± 0.18 kcal mol^{-1} could be estimated at the fluorinated, as grown and oxidized BDD electrodes, respectively. Looking at Figure 11, an important role should be played again by the components of the preexponential factor; this requirement is needed to explain the significantly low exchange current density presently measured at the F−BDD electrode, despite the small value of $\Delta H^{\circ\ddagger}$, comparable with that recorded at the as grown BDD electrode.

To acquire further information on the role of anions for the ferri/ferro cyanide redox couple, the investigation at different temperatures has been carried out also for the system in the HCl media; impedance data have been already shown in Figure 10 and, to complete the picture, kinetic data (in terms of an Arrhenius plot) have been compared with those obtained in sulfuric media and are reported in Figure 12. The catalytic role

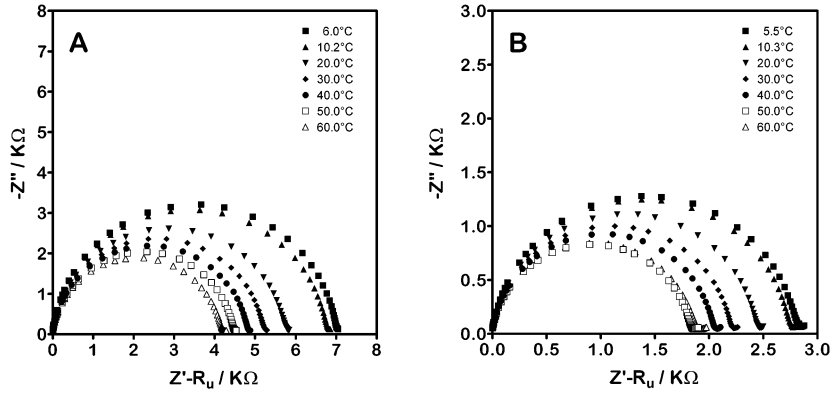

Figure 10. Impedance spectra of 5 mM $Fe[CN]_6^{3-/4-}$ in 0.5 M H_2SO_4 (A) and 1 M HCl (B), recorded at the fluorinated BDD electrode, at different temperatures.

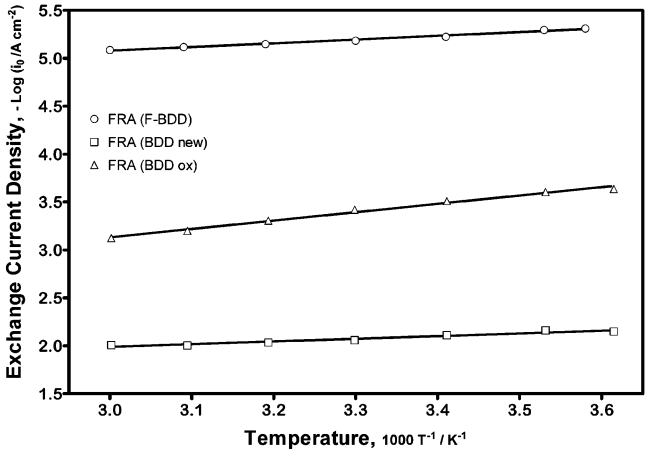

Figure 11. "Arrhenius plot" for the $Fe[CN]_6^{3-/4-}$ redox couple in sulfuric media (comparison with data obtained at *as grown* and *oxidized* BDD[4]).

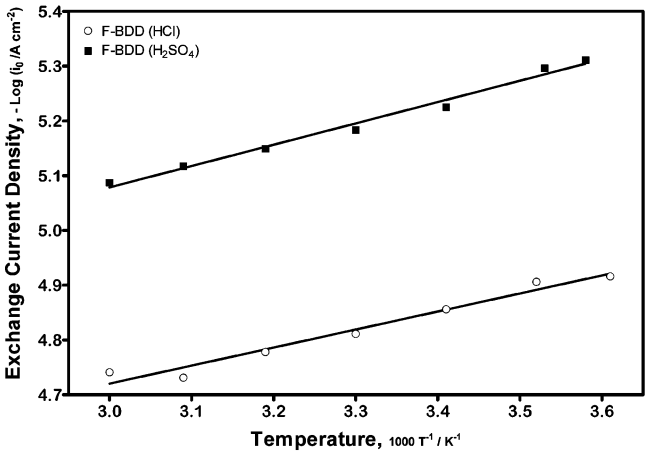

Figure 12. Comparison of "Arrhenius plots" for the $Fe[CN]_6^{3-/4-}$ redox couple in sulfuric and hydrochloric media.

of chlorides is put in evidence by the fact that the activation enthalpy is again more or less the same, while the exchange current density is significantly higher in the presence of Cl^- in solution. Now, the role of the preexponential factor should not be so important (the comparison is made on data obtained at the same electrode material), even if we cannot exclude that some sort of adsorption may affect the electron-transfer process. While no adsorption of charged species has been reported at diamond electrodes so far, such a possibility seems to account for the different data at *unmodified* and *modified* diamond electrodes.

Conclusions

The above data confirm that the near-surface region of diamond thin film electrodes can be modified by fluorination and that such a modification is sufficiently stable, under the conditions explored in the present characterization. XPS analysis, in particular, has shown that the CF_4-plasma treatment results in the formation of a chemical bond between the fluorine and the carbon atoms of the diamond crystals. Unexpectedly, the BDD film appears to be fluorinated not only at its surface but also in the underlying surface region. The available information does not allow defining the detail of the fluorination mechanism: a modification of the surface, followed by surface layer rearrangement, could be, for instance, hypothesized. Otherwise, the growth of a fluorinated diamond film could be a reasonable alternative, essentially leading to the same result. In any case, a fluorination extended to the first tens of nanometers can afford the electrode film a higher stability, compared with a modification strictly limited to the surface.

As far as the electrochemical properties of F−BDD are concerned, the main effect of the surface modification is the extension of the quasi-ideal polarization window due to a shift of about 2 V for the hydrogen evolution reaction, most probably related to a quite low interaction between adsorbed intermediates and fluorinated electrode surface. On the other hand, the electrochemical behavior of MV^{2+}, essentially identical at as grown and F-modified BDD, excludes any influence of changes in charge transport properties caused by the surface fluorination.

The above consideration has to be taken into account also when attempting an explanation for the decrease of k^0 for Eu^{3+}/Eu^{2+} and Fe^{3+}/Fe^{2+} redox couples, amounting to about 1 order of magnitude at the F-terminated surface, compared with values at as grown samples. In these two cases, changes in solvent structure at the electrode/solution interface could be the reason for the observed diminution in the electron-transfer rate. Fe^{3+}/Fe^{2+} data from Arrhenius plots in Figure 9 indicate that this effect may be restricted to the preexponential factor.

Considering the $Fe[CN]_6^{3-}/Fe[CN]_6^{4-}$ redox couple, the value of k^0 decreases almost 3 orders of magnitude when the reaction takes place at the F−BDD electrode. The larger size of these anions and their less important solvation possibly involve an interaction with the inner part of the interfacial region and an extension of the effect to the enthalpy of activation, as can be deduced from the Arrhenius plot in Figure 11. The already observed scarce interaction of the F-terminated surface with hydrogen and hydroxyl radicals implies, in turn, a scarce interaction with water molecules: a hydrophobicity of the electrode surface otherwise expected on the basis of the properties of C−F bond. A primary effect of this would then be an easier organization of the solvent molecules around the reacting species and consequently a slower electron transfer. This effect may be essentially limited to secondary solvation for transition metal cations such as Eu^{3+}/Eu^{2+} and Fe^{3+}/Fe^{2+}. In this connection, it is interesting for instance to remember that k^0 for the Fe^{3+}/Fe^{2+} redox couple at the hydrophobic Au surface is lower than at the more hydrophilic Pt surface.

The above-described results suggest that F-modified BDD may certainly be an interesting material for studies in electrochemical kinetics, offering a substantially unchanged surface through a quite extended ideal polarization range. The stability of C−F bond and the fact that the fluorination of BDD extends for a few nanometers across the near-surface region suggests that this material may exhibit longer service life, e.g., under severe anodic polarization, while the very poor interaction of fluorinated surfaces with hydroxyl and hydrogen radicals suggests interesting applications in electrosynthesis as well as in electrochemical incineration processes. More experimental evidence is necessary to confirm these expectations.

Acknowledgment. The authors are grateful to Dr. M. Dal Colle for carrying out the XPS measurements and to Dr. C. Urgeghe for helpful discussion.

References and Notes

(1) Ferro, S. *J. Mater. Chem.* **2002**, *12*, 2843.
(2) Smentkowski, V. S.; Yates, J. T. U.S. Patent 5,665,435, 1997.
(3) Martin, H. B.; Argoitia, A.; Angus, J. C.; Landau, U. *J. Electrochem. Soc.* **1999**, *146*, 2959.
(4) Ferro, S.; De Battisti, A. *Electrochim. Acta* **2002**, *47*, 1641.

(5) Conway, B. E. Personal communication.
(6) Ferro, S.; De Battisti, A. *J. Electroanal. Chem.* **2002**, *533*, 177.
(7) Zak, J. K.; Butler, J. E.; Swain, G. M. *Anal. Chem.* **2001**, *73*, 908.
(8) Granger, M. C.; Witek, M.; Xu, J.; Wang, J.; Hupert, M.; Hanks, A.; Koppang, M. D.; Butler, J. E.; Lucazeau, G.; Mermoux, M.; Strojek, J. W.; Swain, G. M. *Anal. Chem.* **2000**, *72*, 3793.
(9) Foord, J. S.; Singh, N. K.; Jackman, R. B.; Gutierrez-Sosa, A.; Proffitt, S.; Holt, K. B. *Surf. Sci.* **2001**, *488*, 335.
(10) Alehashem, S.; Chambers, F.; Strojek, J. W.; Swain, G. M.; Ramesham, R. *Anal. Chem.* **1995**, *67*, 2812.
(11) Xu, J.; Granger, M. C.; Chen, Q.; Strojek, J. W.; Lister, T. E.; Swain, G. M. *Anal. Chem.* **1997**, *69*, 591A.
(12) Martin, H. B.; Argoitia, A.; Landau, U.; Anderson, A. B.; Angus, J. C. *J. Electrochem. Soc.* **1996**, *143*, L133.
(13) Kulesza, P.; Jedral, T.; Galus, Z. *J. Electroanal. Chem.* **1980**, *109*, 141.